Polymer Adsorption on Curved Surfaces: A Geometric Approach

ARTICLE *in* THE JOURNAL OF PHYSICAL CHEMISTRY C · AUGUST 2007

Impact Factor: 4.77 · DOI: 10.1021/jp0725073 · Source: PubMed

3 AUTHORS, INCLUDING:

Allen Tannenbaum
Stony Brook University
540 PUBLICATIONS **15,092** CITATIONS
SEE PROFILE

Rina Tannenbaum
Stony Brook University
143 PUBLICATIONS **3,156** CITATIONS
SEE PROFILE

Polymer Adsorption on Curved Surfaces: A Geometric Approach

Eli Hershkovits,[†] Allen Tannenbaum,[†,‡,#] and Rina Tannenbaum*[,£,§]

Schools of Biomedical Engineering, Electrical and Computer Engineering, and Materials Science and Engineering, Georgia Institute of Technology, Atlanta, Georgia 30332, and Departments of Electrical Engineering and Chemical Engineering, Technion, Israel Institute of Technology, Haifa, Israel

Received: March 30, 2007; In Final Form: June 14, 2007

In this article, we have developed a simple model that describes the adsorption of polymer chains from a solution having a good solvent onto a reactive surface of varying curvatures. In order to evaluate the impact of particle size on the adsorption process, we have probed the adsorption of poly(methyl methacrylate) (PMMA) on aluminum oxide (Al_2O_3) surfaces belonging to particles of different sizes. The basic approach assumed that the details of the chemisorption mechanism of PMMA on aluminum oxide surfaces are independent of surface curvature. The combination of the experimental results with the theoretical approach that we have developed show the existence of three different regimes of adsorption of polymer chains onto the surfaces of metal nanoparticles.

1. Introduction

The adsorption of polymers on metallic or metal oxide nanoparticles plays a major role in the control of particle size during polymer-mediated particle synthesis[1−6] and on the characteristics of the particle suspensions in the polymer solutions.[1−7] The adsorbed polymer chains act as a steric and hydrophobic barrier that prevents the aggregation of the metallic clusters beyond an equilibrium size, thus imparting a stabilizing effect on the particle suspension. The extensive, available experimental data regarding the adsorption of polymers on both flat metallic surfaces and on metallic particles can be used to test the various theories that have been developed in this regard[8−12] and to extend the understanding of the polymer adsorption issues to different types of surfaces that differ both in their chemical nature and in their degree of curvature.[13−22]

One of the theories regarding the adsorption of long polymer chains on flat surfaces which was suggested by deGennes uses scaling arguments.[23−25] Mean field calculations were used to extend the solution to this scenario for very small or very large particles and for a finite length of polymers. Molecular dynamics (MD) simulations have given qualitative results for short polymers adsorbed on surfaces. Further, thermodynamic calculations have shown that there is a substantial difference between the adsorption of polymer chains on a surface curved into the bulk of the polymer solution (convex surface) and that curved away from it (concave surface).[26−40] An analytical model of an adsorption process from an ideal polymer solution on large metallic particles has been supported by experimental results and has shown good agreement with these results.[1,7,41−43]

In this Article, we have developed a simple model that is based on scaling arguments to give a solution for the polymer adsorption from a good solvent for a complete range of particle sizes. In order to highlight the specific role that the size of the adsorbing particle imparts on the extent of polymer adsorption, we have limited ourselves to one type of polymer and followed its adsorption on surfaces that differed only in the magnitude of their curvature, that is, from flat surfaces to very small particles consisting of the same chemical makeup. Specifically, we have probed the adsorption of poly(methyl methacrylate) (PMMA), of various molecular weights, on aluminum oxide (Al_2O_3) surfaces belonging to particles of different sizes and length scales.[19−22] The mechanism of reactive adsorption, that is, chemisorption, in this case, is well-understood and well-documented and results in the formation of a coordination bond between the methyl methacrylate (MMA) segments and Al^{+3} sites on the surface. The fundamental premise of our approach was that the details of the chemistry concerning the reactive, segment-level adsorption mechanism of PMMA on aluminum oxide surfaces are independent of surface curvature since the segment-level dimension (the size of the MMA segment is ∼0.5 nm) is at least 1 order of magnitude smaller than the size of the smallest particles probed. Therefore, the variations of the amount of polymer adsorbed and the density of contact points between the polymer and the surface of the particles must be a result of the variations in particle sizes, that is, of surface curvature. Our work incorporates results obtained from adsorption experiments into the scaling model that we have developed and, thus, probes the validity of the model and its predictive capability.

2. Experimental Section

2.1. Experimental Procedure. *2.1.1. Preparation of Initial System Mixtures.* A volume of 220 mL of chlorobenzene 99+% (Acros, density 1.106 g/cm^3) was introduced into a 500 mL Erlenmeyer flask, which was placed on a Thermolyne Mirak stirring hotplate with the temperature set to 70 °C. A magnetic stirrer was dropped into the flask and began spinning at the preset speed of 200 RPM. An amount of 32.48 g of poly(methyl methacrylate), PMMA, (Aldrich Chemical Co., Inc., $\bar{M}_w$ of

* To whom correspondence should be addressed. E-mail: rinatan@mse.gatech.edu.
† School of Biomedical Engineering, Georgia Institute of Technology.
‡ School of Electrical and Computer Engineering, Georgia Institute of Technology.
£ School of Materials Science and Engineering, Georgia Institute of Technology.
Department of Electrical Engineering, Technion, Israel Institute of Technology.
§ Department of Chemical Engineering, Technion, Israel Institute of Technology.

10.1021/jp0725073 CCC: $37.00
Published on Web 08/02/2007 PAGE EST: 6.9

330 000 g/mol, density 1.170 g/cm^3) was poured into the flask to form a 1.175 wt % PMMA solution. After the polymer was completely dissolved, the stirrer was removed. Next, 0.50 grams of alumina (Al_2O_3) nanoparticles (Nanophase Technologies, D_{avg} = 39 nm, density 1.77 g/cm^3) was measured and kept in weighing paper. The flask was agitated on a Scientific Industries Vortex-2 Genie vortex with a setting of 8−10. While the mixture was swirling continuously, the alumina was slowly poured into the flask. Mixing continued for 5 min. The flask was covered with laboratory film and stored in a fume hood for 24 h. Similar experiments were performed with PMMA (Alfa Aesar) of other molecular weights, that is, $\bar{M}_w$ = 60 000, 120 000, or 250 000 g/mol, (first one with PDI = 1.04 and the last two with PDI = 1.12), and other sizes of the alumina particles, that is, D_{avg} = 4, 97, 400 nm. Pure PMMA reference samples were created using 32.48 g of PMMA in 110 mL of chlorobenzene.

Experiments on flat alumina surfaces were performed by first depositing a 1000 Å layer of aluminum onto previously washed Si wafers by electron beam evaporation, using an instrument equipped with a multisample holder mounted on a rotating carriage to ensure even deposition. The thickness of the metal film was measured with a quartz crystal monitor. Immediately upon removal from the evaporator, the freshly prepared aluminum substrates were immersed in a 1.175 wt % chlorobenzene solution of PMMA. The time lapse from the opening of the sample holder of the evaporator and the complete immersion of the samples in the PMMA solution was, on the average, less than 10 min. This allowed the formation of an amorphous native oxide layer on the aluminum surface.[20,22] The PMMA solutions with the immersed metal oxide substrates were left in the PMMA solution under inert atmosphere and at room temperature for 24 h. Excess, unadsorbed PMMA was removed by repeated washing with chlorobenzene to generate a stable, chemisorbed PMMA film.

2.1.2. Characterization of Alumina Particle Size. Transmission electron microscopy (TEM) was used to determine the size and distribution of original particles for all polymer nanocomposite systems. TEM samples were obtained by placing a small droplet of the reacted solution containing the polymer-coated metal oxide particles onto a Formvar coated copper TEM grid from Ted Pella. The grid rested on a thin piece of tissue paper so that the liquid would drain into the paper, leaving a very thin film on the grid itself. The TEM analysis was performed on a JEOL 4000EX high-resolution electron microscope with an operating voltage of 200 keV.

2.1.3. Characterization of the Adsorbed Polymer Layer. Thermo gravimetric analysis (TGA) was conducted to measure the thickness of the polymer interphase. TGA samples were prepared by centrifuging each of the polymer nanocomposite mixtures using Fisher Scientific Centrific Model 228 centrifuge at 10 000−15 000 RPM for 12−17 min. The capped particles formed a solid mass at the bottom of the vial, and excess polymer and solvent solution were removed. The remaining particles were washed with solvent, and the vial was shaken using a Scientific Industries Vortex-2 Genie vortex for 1 min to remove any excess unbound polymer from the particles. The suspension was centrifuged again, and this process was repeated 3−4 times. The particles were placed onto a TGA platinum pan, and the data were collected using a TA Instruments Inc. TGA Model 50 at a ramp rate of 10 °C/min to 600 °C.

FTIR was used to identify the bonding between the polymer chains and nanoparticles in the various Al_2O_3−PMMA nanocomposite systems that we explored. The sample cell was placed inside a Nicolet Instrument Corporation Nexus 870 FT-IR spectrometer sample compartment, and after the latter was sealed and purged for at least 15 min, background spectra were taken and assigned for use on subsequent spectra acquisitions. The vials containing the centrifuged capped particles were shaken using a Scientific Industries Vortex-2 Genie vortex to initiate their resuspension in a hydrocarbon solvent. Using Nicolet OMNIC 5.2a software, the spectra of the capped metal oxide particles were compared against previously recorded spectra of PMMA solutions or PMMA thin films to highlight peaks that are unique to the capped particles.

Determination of polymer layer thickness was performed using a J. A. Woollam Co. Inc. variable-angle spectroscopic ellipsometer (VASE). Prior to the adsorption process, the optical parameters of the bare metal oxide layer and the refractive index of a spin-coated (nonadsorbing) PMMA film were determined. The PMMA film thickness at various different points on the substrate and for two different angles of incidence was determined to be ~87 ± 8 Å. The film was thin enough to see the photoemission signal and/or avoid distortions of the vibrational band shapes that depend on the thickness and refractive index of the sample.

2.2. Calculation of Anchoring Density. The number of chains in the sample is given by the following expression

$$N_{chains} = \frac{M_{sample} \cdot w_{polymer} \cdot N_A}{\bar{M}_w} \quad (1)$$

where M_{sample} is the mass of the sample, $w_{polymer}$ is the mass fraction of polymer as determined from TGA data, and $\bar{M}_w$ is the weight-average molecular weight of the polymer. Similarly, TGA data were used to calculate the number of oxide clusters in the sample according to the following expression

$$N_{clusters} = \frac{M_{sample} \cdot w_{cluster}}{d \cdot (4\pi/3)(D_{cluster}/2)^3} \quad (2)$$

where $w_{cluster}$ is the mass fraction of the alumina clusters as determined from TGA measurements, d is the density of the alumina nanoclusters, and $D_{cluster}$ is the average diameter of the alumina clusters as determined from TEM measurements.

The first step in the bonding process between the PMMA chain segments and Al_2O_3 nanoparticles is the hydration of the alumina cluster to form a monolayer of oxy−hydroxide surface groups[19−22,44]

$$Al_2O_3 + H_2O \rightleftarrows 2AlO(OH) \quad (3)$$

In the second step, the presence of the OH group on the nanoparticle surface facilitates hydrolysis of the PMMA ester group to produce either a COOH acid group or its conjugate COO^- base group, according to the following reaction[19−22]

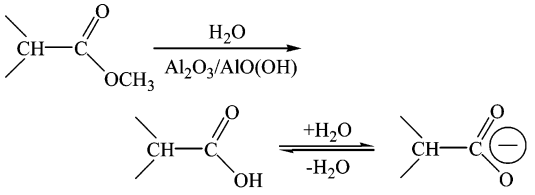

(4)

The COO^- group directly interacts with the positively charged Al(III) atoms to generate a bond between the polymer segment and the aluminum oxide nanoparticle surface.[20,22] This bonded segment is an anchoring point for the PMMA chain.

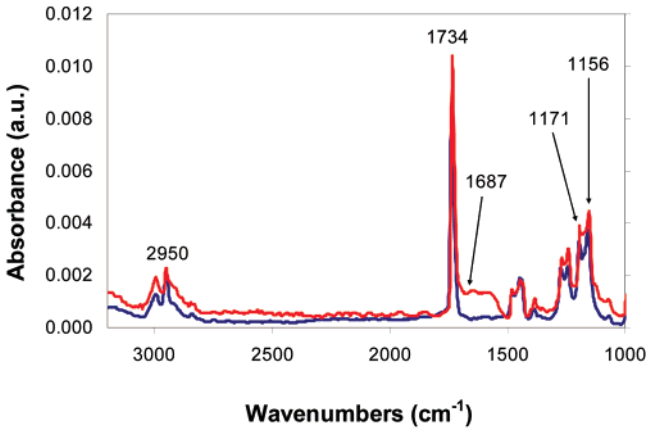

Figure 1. The infrared spectra of PMMA before (blue) and after (red) its interactions with the aluminum oxide surface. The comparison between the two spectra reveals several changes, (a) the decrease in the absorbance of the 2950 cm^{-1} peak, which corresponds to the hydrolysis of some of the methoxy groups in the adsorbed PMMA, (b) a relative increase of the 1687 cm^{-1} peak as compared to the 1734 cm^{-1} carbonyl peak, which corresponds to the asymmetric stretch of the COO^- groups, and (c) a reversal of the relative intensities of the 1156 and 1171 cm^{-1} infrared absorption bands, which corresponds to the cooperative symmetric and asymmetric stretches of the C−O and C−C bonds of the polymer backbone, indicating changes in the conformation of the polymer chains upon adsorption.

The changes in the infrared spectra of PMMA resulting from its interactions with the oxide surface are shown in Figure 1. The decrease in the absorbance of the 2950 cm^{-1} peak corresponds to the hydrolysis of some of the methoxy groups in adsorbed PMMA, as indicated in the first reaction of eq 2. The second and third reactions of eq 2 are characterized by a relative increase of the 1687 cm^{-1} peak, corresponding to the asymmetric stretch of the COO^- group,[20,22] as compared to the 1734 cm^{-1} carbonyl peak for the adsorbed PMMA. Hence, the ratio $(COO^-/C{=}O) = (E_{1687}/E_{1734})$ provides the relative concentration of the reacted COO^- group.[20,22,45] The reactive adsorption of PMMA on the surface of the metal oxide nanoparticles through direct bonding of segments requires a change in the conformation of the polymer.[20,22,45] These conformation rearrangements in the polymer generate a reversal of the relative intensities of the 1156 and 1171 cm^{-1} infrared absorption bands, corresponding to the cooperative symmetric and asymmetric stretches of the C−O and C−C bonds of the polymer backbone. The ratio of these two bands indicates the proportion of polymer segments that experience the conformational changes indicative of the bonding process. The total number of PMMA carboxylate groups that have undergone hydrolysis and have anchored to the surface can be calculated from the ratio of the fraction of the segments containing the bonding group (COO^-) experiencing the conformational change multiplied by the total number of monomers in the sample. Dividing this by the total number of chains gives the number of anchoring points per chain[20,22,45]

$$\frac{\text{Anchors}}{\text{Chain}} = \frac{E_{1687}}{E_{1734}} \cdot \frac{E_{1156}}{E_{1171}} \cdot \frac{N_{\text{monomers}}}{N_{\text{chains}}} \tag{5}$$

The density of the chains adsorbed on the surface of the aluminum oxide nanoclusters, η, is given by

$$\frac{N_{\text{chains}}}{A_{\text{clusters}}} = \frac{w_{\text{polymer}} \cdot N_A \cdot d \cdot (D_{\text{cluster}}/2)}{3 \cdot w_{\text{cluster}} \cdot \bar{M}_w} \tag{6}$$

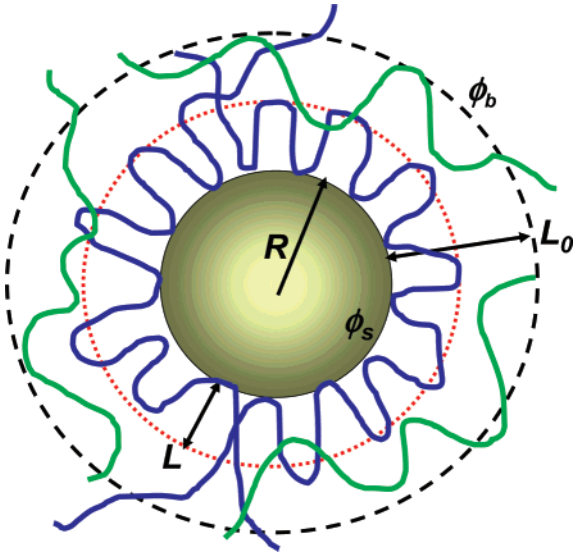

Figure 2. Schematic representation of the polymer chains adsorbed from a semidilute solution onto a spherical particle with radius R. The chains of the adsorbed polymers form two adsorption shells, (a) a layer with a width L that has a constant radial distribution of monomers; we will refer to this shell as the "adsorption shell" and (b) a layer with a width L_0 in which the concentration of the monomers decreases from the adsorption concentration on the inner sphere to the bulk concentration on the outer shell. This is referred to as the "depletion shell".

Combining eqs 5 and 6 gives the density of anchoring points per unit area of oxide nanocluster surface (in units of nm^2), σ.

3. The Model

In order to simplify the calculations, we have relied on the following assumptions: (a) The solvent in the system is a good solvent for the polymer; (b) the polymer chains adsorb to metallic particles with spherical geometry, irrespective of their size; (c) the concentration of the bulk polymer solution is in the dilute/semidilute regime; (d) the polymer is a linear and flexible chain and exhibits a random coil conformation in the good solvent; and (e) the monomer adsorption energy, δ, is smaller than the thermal energy, or if we normalize the adsorption energy by the thermal energy k_BT (where k_B is the Boltzmann constant and T is the absolute temperature), we get $\delta \ll 1$. This is the weak adsorption assumption.[22−25]

A schematic description of the adsorption process is sketched in Figure 2. The polymers next to the surface form an adsorption layer with a typical width L. As a consequence of the weak adsorption, the coverage of the surface by monomers is low, and the solution next to the adsorbing surface is in the semidilute region.

Polymer adsorption on surfaces is a process that is determined by two competing processes. The first is the contraction of monomers to the surface due to the adsorption interaction of the monomers with the surface. The second is the entropic repulsion between the monomers that are confined to the surface vicinity. The first process is determined directly by the adsorption constant. The second process is modeled based on an equivalence hypothesis between the adsorption process to a surrogate problem of a polymer solution confined between two desorbing boundaries.[23−25]

The resulting free energy in the adsorption layer (normalized by the thermal energy) is $F_c = E_{con} - N_c\delta$, where N_c is the total number of monomers adsorbed onto the surface and E_{con} is the confinement energy.

We now want to examine the geometric properties of the above expression for the free energy in the adsorption layer.

First, we adopt the conventional form of the confinement energy of a polymer in a good solvent, $E_{con} = (R_f/L)^{5/3} = N(a/L)^{5/3}$, where $R_f = N^{3/5}a$ is the gyration radius of the polymer in a good solution,[23−25] N is the number of monomers in a polymer, and a is the monomer size. This expression is deduced via scaling arguments, where it is assumed that the confinement energy of a polymer scales with N. The same expression was used to express the free energy of a polymer in solution next to an adsorbing sphere.[1] The total number of adsorbed monomers on a sphere of radius R is $N_c = 4\pi(R^2/a^2)\phi_s$, where ϕ_s is the volume fraction of the monomers next to the surface of the sphere. Substituting these results into the expression for the adsorption free energy gives

$$F_c = nN\left(\frac{a}{L}\right)^{5/3} - 4\pi\left(\frac{R^2}{a^2}\right)\delta\phi_s \tag{7}$$

where n is the number of the polymers adsorbed onto the sphere.

Asumming that the volume fraction is constant in the adsorption layer, ϕ_s can be expressed as a function of the width of the adsorption layer

$$\phi_s = \frac{3nNa^3}{4\pi[(R+L)^3 - R^3]} \tag{8}$$

For a particle where $R \gg L$ (small curvature), the denominator simplifies to $12\pi R^2 L$, and the free energy is

$$F_c = (nN)^{-2/3}(4\pi)^{5/3}\left(\frac{R^2}{a^2}\right)^{5/3}\phi_s^{5/3} - 4\pi\left(\frac{R^2}{a^2}\right)\delta\phi_s \tag{9}$$

To simplify the model, we are assuming that the surface concentration term is correlated with the geometry and with the adsorption strength better than the other variables in the problem. In the next section, we will use the experimental results to extend the model to include also the variability in the number of polymers adsorbed onto the surface.

According to this simplification, the volume fraction of the monomers next to the surface can be found by minimization of the energy with respect to ϕ_s to give the following

$$\phi_s = \left(\frac{3}{5}\right)^{3/2}\left(\frac{1}{4\pi}\right)\left(\frac{a}{R}\right)^2 nN\delta^{3/2} \tag{10}$$

This expression shows the predicted 3/2 power law dependence of the volume fraction on the adsorption constant δ.[23−25]

Using the same arguments in the case of particles with high curvature, $R \ll L$, we obtain

$$\phi_s = nN\left(\frac{a^2}{R^2}\right)^{9/4}\delta^{-9/4} \tag{11}$$

The resulting equilibrium coverage volume fraction increases when the adsorption constant decreases. This conclusion seems to be counterintuitive. In the low coverage region, we can expect that the coverage will increase with the adsorption strength. This result seems to indicate that the model has to be altered in order to accommodate the effect of the curvature of the adsorbing particle.

We will argue that the above model (eqs 7 and 8) should be modified in a manner that emerges from the difference in geometry. First, the conformational energy term might be geometry dependent. Second, the number of polymers adsorbed on a single particle, n, might show a nontrivial dependence on the adsorbing particle geometry.

As for the confinement energy term, it was shown by Sakaue and Raphael[8] that the expression for the energy of a particle confined in a cylinder or in a slit is substantially different than that for a polymer confined in a sphere. In the general case, a polymer confined in one or two dimensions has different confinement energy than that of a polymer which is confined in three dimensions.[8,29,30] The argument for this difference in behavior is that while in the slit and in the cylinder an increase of the polymer length does not change the volume fraction of the confined polymer, inside of a sphere, the same change will cause the volume fraction to increase. To get the correct expression for the energy of a polymer confined inside of a sphere, we have to take into consideration that the volume of the polymer scales as the polymer length, and hence, the pressure ($P = -\Delta F/\Delta V$) is constant when the length and the volume of the polymer scale in the same manner. On the basis of this scaling argument, the thermally normalized free energy of polymers in a good solvent confined inside a sphere of radius L is

$$E_{con} \cong (nN)^{9/4}\left(\frac{a}{L}\right)^{15/4} \cong nN\phi_s^{5/4} \tag{12}$$

The second equality is deduced from eq 8 by introducing the condition that $L \gg R$, which is the case when the particles are very small (i.e., the surface curvature is very high). This expression is substantially different than the confinement free energy result we used in eq 7.

We have used the equivalence hypothesis for the confinement energy of the polymers to get the free energy in the adsorption layer next to a small sphere

$$F_c = nN\phi_s^{5/4} - 4\pi\left(\frac{R^2}{a^2}\right)\delta\phi_s \tag{13}$$

Minimizing the free energy with respect to the volume fraction on the surface then gives the following expression

$$\phi_s \propto (nN)^{-4}\left(\frac{R^2}{a^2}\right)^4\delta^4 \tag{14}$$

Here, the surface volume fraction of the polymer increases with δ, as should be expected. We would like to remark that this expression would be altered significantly in the case of a theta solvent. For this case, the power of δ and of $(1/nN)$ in eq 14 will be changed from 4 to 1. Such a modification of the surface concentration should be noticeable in an appropriate experiment.

Thus far, we have only considered possible modification to the model via alterations to the confined energy term in eq 9. Additional changes in the adsorption might accrue if the variables of the model have an explicit dependency on the geometry of the adsorbing metal particles or on the adsorption strength. For example, the number of the polymers adsorbed to a sphere of radius R should be proportional to the sphere area or to R^2 in the trivial case in which the adsorption process is curvature independent. More complicated curvature dependency can be expected[26] and will contribute to the modification of the results for adsorption on small particles. The experiment that we are presenting was designed to check the geometric dependency of the density parameters in the adsorption layer and on the particle surface.

4. Results and Discussion

Two different characterization methods have yielded two types of experimental data: (a) The number of anchoring points

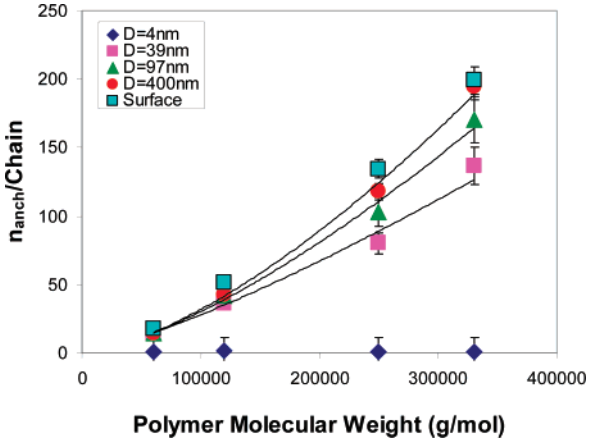

Figure 3. The number of anchoring points (i.e., surface-bound monomers) per polymer chain adsorbed on the cluster surface, as calculated from FTIR experimental data (according to eq 5 in the text).

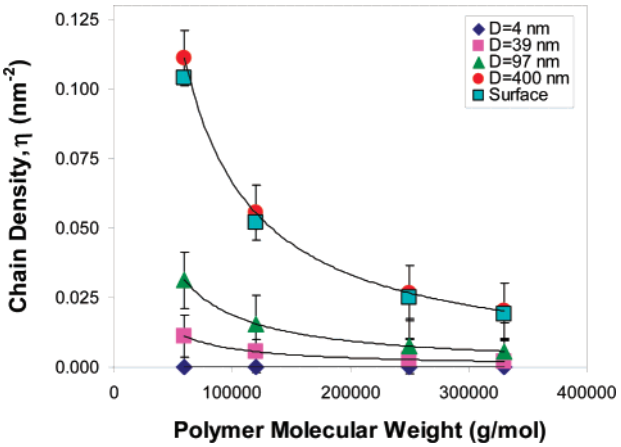

Figure 4. The number of adsorbed polymer chains per unit area of cluster surface (in units of nm^2), η, as calculated from TGA experimental data (according to eq 6 in the text).

(i.e., surface-bound monomers) per polymer chain adsorbed on the cluster surface was obtained from FTIR experiments according to eq 5, as shown in Figure 3 and (b) the number of adsorbed polymer chains per unit area of cluster surface (in units of nm^2), η, was obtained from TGA experiments according to eq 6, as shown in Figure 4. The combination of these two independent experiments yielded the density of the number of anchoring points per unit area of cluster surface (in units of nm^2), σ, and is shown in Figure 5. These latter two parameters can be related to each other with the formula

$$\sigma = \frac{3a\eta NR^2}{(R+L)^3 - R^3} \tag{15}$$

where σ is the number of monomers anchored to the metal surface per nm^2, a is the lattice dimension or the typical PMMA monomer, which is approximately 0.5 nm, R is the average radius of the metallic spherical nanoparticle, N is the polymer length (i.e., the number of segments), η is the number of polymers adsorbed per nm^2 of the metallic particle surface, and L is the thickness of the polymers adsorption layer. Within this layer, the concentration of monomers is assumed to be almost constant. The planar concentration of monomers in the adsorption layer, Γ ($\Gamma = \eta N$), does not depend on the polymer length, only on the metallic cluster radius, as shown in Table 1.

When the thickness of the adsorption layer is much smaller than the cluster radius, that is, $L/R \ll 1$, eq 15 simplifies to the

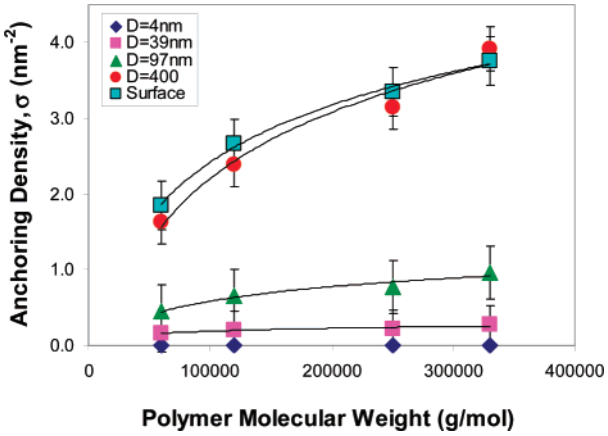

Figure 5. The number of anchoring points per unit area of cluster surface (in units of nm^2), σ, as calculated by the combination of the independent experimental results obtained from FTIR and TGA (values from eq 5 multiplied by the values from eq 6 for the corresponding polymers and particles).

TABLE 1: Summary of the Total Number of Monomers Per Unit Area, Γ, as a Function of Polymer Length, *N* (Polymer Degree of Polymerization), and Average Particle Size, *D* (in nm)[a]

D_{avg}	$N = 600$	1200	2500	3300
4 nm	0.12	0.11	0.11	0.11
39 nm	6.6	6.6	6.75	6.6
97 nm	18.66	18.72	18.75	18.81
400 nm	66	66	66.5	66
surface	62.4	62.4	62.25	62.37

[a] Note that $\Gamma = N{\cdot}\eta$, where η is the number of polymer chains adsorbed per unit area (in nm^2) of cluster surface. As can be seen, Γ does not depend on N but only on D.

TABLE 2: Correction to the Finite Degree of Polymerization in the Adsorption Layer Width, ΔL_M (as Per Eq 16 in the Text), as a Function of Polymer Length, *N* (Polymer Degree of Polymerization), and Average Particle Size, *D* (in nm)[a]

D_{avg}	$N = 600$	1200	2500
39 nm	−17	−9.2	−7.2
97 nm	−22.8	−9.53	−5
400 nm	−23.5	−10	−4.1
surface	−17	−7.24	−2

[a] This correction gives the difference between the widths of the adsorption layer for a polymer with finite length and a polymer with infinite length. The experimental value of $M = 3300$ (corresponding to M_w of 330 000 g/mol) already gives a result that is close to the case with an infinite degree of polymerization.

following expression, $\sigma = a\eta N/L$. From this, we get the expression for the adsorption layer width for polymers with degree of polymerization N

$$L_{(M)} = \frac{a\eta M}{\sigma_{(M)}} = \frac{a(\eta{\cdot}N)_{N\to\infty}}{\sigma_{(N)_{N\to\infty}}} - \Delta L \tag{16}$$

We set $M = 3300$ (corresponding to a molecular weight of 330 000 g/mol) to be a polymer length where the behavior of the polymer is close to that of an infinitely long polymer ($N \to \infty$). The first observation is that $L_{(3300)}$ converges to a constant when we increase the metal cluster radius, and the experimental limit is $L = 9$ nm. When we substitute the values from Figures 3 and 4 into eq 16, we can get ΔL as a function of N and R. The results are summarized in Table 2. As can be seen, $\Delta L_{(N)}$ is proportional to $1/N$. This behavior agrees with the relevant theoretical prediction.[1,45]

TABLE 3: Scaling of the Planar Densities Γ and σ with 1/R (where R is the Average Radius of the Adsorbing Particles) as a Function of Average Particle Size, D (in nm)

D_{avg}	$\eta N/R$	σ/R
39 nm	0.17	0.0071
97 nm	0.192	0.01
400 nm	0.165	0.0098

An interesting observation that follows from the experimental result is that both planar densities σ and η scale with the curvature 1/R, as shown in Table 3. This scaling emerges from the fact that the adsorption of polymer chains on surfaces which are not flat is inherently influenced by geometric constraints. To see this, we schematically describe the adsorption on a flat surface, shown in Figure 6, versus adsorption onto a spherical surface, shown in Figure 7. On the flat surface, the monomer concentration, ϕ_s, is approximately constant in the adsorption layer. Then, the concentration decreases down to the distance L_0, at which distance it becomes equal to the bulk concentration ϕ_b. The adsorption energy per unit of surface is responsible for the concentration gradient. While this is straightforward for the planar geometry, in the spherical geometry, there is an additional decrease in the density of the polymer chains (coils) that is inversely proportional to the difference between the area of the cluster and that of the larger sphere in which the bulk adsorbed concentration is achieved. This difference is $A_{(R+L_0)} - A_{(R)} \approx (dA_{(R)}/dr) \approx R$ when L_0 is sufficiently small. Hence, the same adsorption energy can support a smaller concentration gradient along L_0, and this term scales with the curvature 1/R. This is true for L_0, which we assume to be of the same order of L for smaller cluster radii.

We can now extract the adsorption strength from the parameters that were measured in the experiment. To see this, we have to write the explicit expression of the free energy of the adsorbed monomers. We employ the expression that was devised for a semidilute polymer solution in a good solvent for a weak monomer adsorption[23−25]

$$f_c = \eta\left(\frac{R_f}{L}\right)^{5/3} - \delta\sigma \qquad (17)$$

where f_c is the free energy of the monomers normalized by the thermal energy, R_f is the Flory radius of the polymer, $R_f = aN^{3/5}$, and δ is the strength of the interaction between the alumina and the PMMA monomers, normalized by the thermal energy as well.

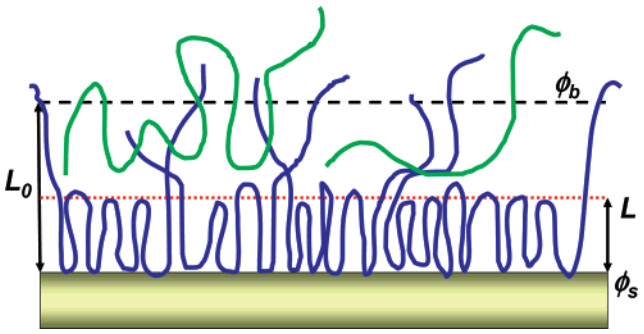

Figure 6. Schematic representation of polymer adsorption on a flat surface. The minimal coil size between two adjacent anchoring points defines the width of the adsorption layer L. The concentration of the monomer in this layer, ϕ_s, is constant. The longer the coils are, the less abundant they will be in the proximity of the surface, and hence, the concentration of the monomers will decrease from ϕ_s at a distance L from the surface to the bulk concentration ϕ_b at a distance L_0 from the surface.

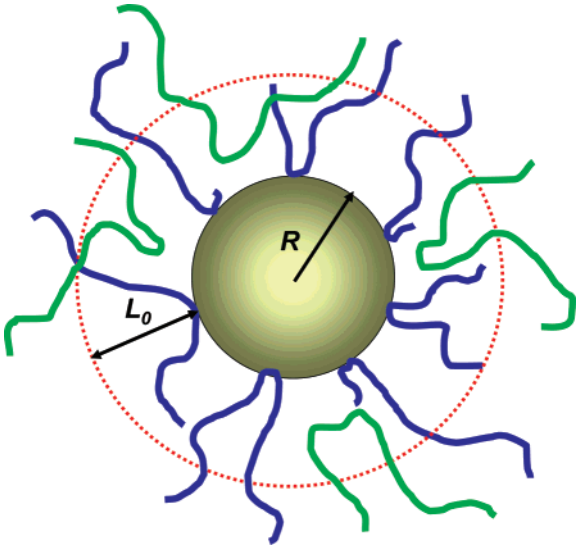

Figure 7. Schematic representation of polymer adsorption on a small spherical particle. For a spherical surface, the depletion in the monomer concentration will have a stronger gradient from the adsorption concentration to the bulk concentration because the farther the coils are from the surface, the larger the distance between them will be. The only way to reduce this gradient is to reduce the density of the adsorbed monomers. This can be achieved if the adsorbed polymers will be further stretched outward away from the adsorbing particles, thus reducing the density of the adsorbed monomers as much as possible. Hence, for adsorbing particles with very small R, the depletion width L_0 becomes smaller than the width of the adsorption layer L. Nonanchored (physisorbed) polymer chains will penetrate into the depletion layer to equilibrate the density in the proximity of the surface to the densities in the bulk, without actually adsorbing to the surface, rendering this process highly dynamic.

Substituting the expression we have developed for L in eq 16 into eq 17, we derive

$$f_c = (\eta N)^{-2/3}\sigma^{5/3} - \delta\sigma \qquad (18)$$

To get a minimum for the free energy as a function of the concentration, we differentiate eq 18 with respect to the density and set the result to zero, obtaining the following

$$\sigma = (3/5)^{3/2}\eta N\delta^{3/2} \qquad (19)$$

From this expression, we can extract the adsorption strength

$$\delta = (3/5)\left(\frac{\sigma}{\eta N}\right)^{2/3} \qquad (20)$$

Substituting the parameters that were generated by the experimental data into eq 20, we find that $\delta = 0.1$. When we multiply this value by the thermal energy (at room temperature), we find that $\delta \approx 0.05$ J. This value for the adsorption energy is well within the weak adsorption limit and is consistent with the assumptions that we have made.

5. Conclusions

Our experimental results in conjunction with the theoretical approach that we have developed have allowed us to establish three different regimes of adsorption of polymer chains onto the surfaces of metal nanoparticles: (a) Large clusters: When the cluster radius is much larger than the radius of gyration of the polymer, the adsorption is similar to adsorption on a flat metal surface. (b) Medium clusters: When the cluster size is on the order of magnitude of the radius of gyration of the

polymer, geometrical constraints force the scaling of the adsorbed monomer densities with the curvature. In this case, the thickness of the adsorbed polymer layer is similar to the thickness of the adsorbed layer on a flat surface. (c) Small clusters*:* When the radius of the cluster is on the same order of magnitude as the thickness of the adsorbed layer, the curvature is too large to support an energy gradient between the adsorbed layer and the bulk. As a result, the adsorbed polymer chains will extend outwardly from the surface of the cluster in order to decrease the density gradient. This will impose an upper bound of unity on the number of anchoring points per polymer chain per cluster. It will also cause a penetration of nonadsorbed polymer chains into the adsorption layer (Figure 7). The clusters will therefore be enveloped by a mixture of adsorbed polymer chains that extend outward into the solution and entangled polymer chains from the solution.

These results have important implications regarding the synthesis avenues and the potential enhancement of the properties of nanocomposite materials, in which nanoscale metallic particles are embedded in polymer matrices. We have shown, in this work, that the morphology of the interfacial region between the nanoparticles and the adsorbed polymer layer is strongly dependent on the size of the nanoparticles and the relationship between this size and the thickness of the adsorbed layer. Hence, since the interface in nanocomposites is the region that facilitates the transport of energy across the material, its morphology will play a crucial role in the extent of property enhancement that we can expect.

Acknowledgment. This work was supported, in part, by grants from NSF, AFOSR, ARO, MURI, MRI-HEL, as well as by a grant from NIH (NAC P41 RR-13218) through Brigham and Women's Hospital. This work is part of the National Alliance for Medical Image Computing (NAMIC), funded by the National Institutes of Health through the NIH Roadmap for Medical Research, Grant U54 EB005149. Information on the National Centers for Biomedical Computing can be obtained from http://nihroadmap.nih.gov/bioinformatics. Allen Tannenbaum is also with the Department of Electrical Engineering, Technion, Israel, where he is supported by a Marie Curie Grant through the European Union (EU). This research was also supported by the National Science Foundation, Grant No. 0704006, and by the National Institute of Health, through the Centers of Cancer Nanotechnology Excellence: Emory−GT Nanotechnology Center for Personalized and Predictive Oncology, Award No. 5-40255-G1: CORE 1. Rina Tannenbaum is also with the department of Chemical Engineering, Technion, Israel, where she is supported by a Marie Curie Grant through the European Union (EU) and by the Israel Science Foundation, Grant No. 650/06.

References and Notes

(1) Tadd, E.; Zeno, A.; Zubris, M.; Dan, N.; Tannenbaum, R. *Macromolecules* **2003**, *36*, 6947−6502.
(2) Tannenbaum, R.; Zubris, M.; Goldberg, E. P.; Reich, S.; Dan, N. *Macromolecules* **2005**, *38*, 4254−4259.
(3) Dan, N.; Zubris, M.; Tannenbaum, R. *Macromolecules* **2005**, *38*, 9243−9250.
(4) Wijmans, C. M.; Zhulina, E. B. *Macromolecules* **1993**, *26*, 7214−24.
(5) Gittins, D. I.; Caruso, F. *J. Phys. Chem. B* **2001**, *105*, 6846−6852.
(6) Piirma, I.; Chen, S. R. *J. Colloid Interface Sci.* **1980**, *74*, 90−102.
(7) Dan, N. *Langmuir* **2000**, *16*, 4045−4048.
(8) Sakaue, T; Raphael, E. *Macromolecules* **2006**, *39*, 2621−2628.
(9) O'Shaughnessy, B.; Vavylonis, D. *J. Phys.: Condens. Matter* **2005**, *17*, R63−R99.
(10) Johner, A.; Semenov, A. N. *Eur. Phys. J. E* **2002**, *9*, 413−416.
(11) Joanny, J.-F. Interactions of polymers in solution with surfaces. In *Handbook of Adhesive Technology*, 2nd Ed.; Pizzi, A., Mittal, K. L., Eds.; Marcel Dekker, Inc.: New York, 2003, pp 145−157.
(12) Dan, N. *Macromolecules* **1994**, *27*, 2310−2312.
(13) Brown, H. R. *Mater. Forum* **2000**, *24*, 49−58, and pertinent references therein.
(14) Jackman, R. J.; Brittain, S. T.; Adams, A.; Wu, H.; Prentiss, M. G.; Whitesides, S.; Whitesides, G. M. *Langmuir* **1999**, *15*, 826−836.
(15) Grunze, M.; Hahner, G.; Woll, Ch. *Surf. Interface Anal.* **1993**, *20*, 393−401.
(16) Netz, R. R.; Andelman, D. *Surf. Sci. Series* **2001**, *103*, 115−155 (Oxide Surfaces).
(17) Ho, P. S. *Appl. Surf. Sci.* **1985**, *41*−*42*, 559−566, and pertinent references therein.
(18) Zazzera, L.; Tirrell, M.; Evans, J. F. *J. Vac. Sci. Technol., A* **1993**, *11*, 2239−2243.
(19) Tannenbaum, R.; Hakanson, C.; Zeno, A. D.; Tirrell, M. *Langmuir* **2002**, *18*, 5592−5599.
(20) Kostandinidis, F.; Thakkar, B.; Chakraborty, A. K.; Potts, L.; Tannenbaum, R.; Tirrell, M.; Evans, J. *Langmuir* **1992**, *8*, 1307−1317.
(21) King, S.; Hyunh, K.; Tannenbaum, R. *J. Phys. Chem. B* **2003**, *107*, 12097−12104.
(22) Tannenbaum, R.; King, S.; Lecy, J.; Tirrell, M.; Potts, L. *Langmuir* **2004**, *20*, 4507−4514.
(23) De Gennes, P. G. *Macromolecules* **1981**, *14*, 1637−1644.
(24) De Gennes, P. G. *Adv. Colloid Interface Sci.* **1987**, *27*, 189−209.
(25) De Gennes, P. G. *J. Phys. (Paris*) **1976**, *37*, 1445−1452.
(26) Ji, H; Hone, D. *Macromolecules* **1988**, *21*, 2600−2605.
(27) Nowicki, W. *Macromolecules* **2002**, *35*, 1424−1436.
(28) Skau, K. I.; Blokhuis, E. M. *Macromolecules* **2003**, *36*, 4637−4645.
(29) Gorbunov, A. A.; Zhulina, E. B.; Skvortsov, A. M. *Polymer* **1982**, *23*, 1133−1142.
(30) Brochard-Wyart, F.; Tanaka, T.; Borghi, N.; de Gennes, P.-G. *Langmuir* **2005**, *21*, 4144−4148.
(31) Kim, Y. W.; Sung, W. *Phys. Rev. E* **2001**, *63*, 041910/1−041910/5.
(32) Haronska, P.; Vilgis, T. A.; Grottenmueller, R.; Schmidt, M. *Macromol. Theory Simul.* **1998**, *7*, 241−247.
(33) Carignano, M. A.; Szleifer, I. *J. Chem. Phys.* **1995**, *102*, 8662−8669.
(34) Striolo, A.; Jayaraman, A.; Genzer, J.; Hall, C. K. *J. Chem. Phys.* **2005**, *123*, 064710/1−064710/15.
(35) Baschnagel, J.; Johner, A.; Joanny, J.-F. *Eur. Phys. J. B* **1998**, *6*, 45−55.
(36) Marla, K. T.; Meredith, J. C. *Langmuir* **2005**, *21*, 487−497.
(37) Metzger, S.; Muller, M.; Binder, K.; Baschnagel, J. *Macromol. Theory Sim*ul. **2002**, *11*, 985−995.
(38) Sikorski, A. *Macromol. Theory Simul.* **2002**, *11*, 359−364.
(39) Douglas, J. F.; Freed, K. F. *Macromolecules* **1997**, *30*, 1813−1817.
(40) Shi-Ben, L; Lin-Xi, Z. *J. Polym. Sci., Part B: Polym. Phys.* **2006**, *44*, 2888−2901.
(41) Aubouy, M. *Phys. Rev. E* **1997**, 56, 3370−3377.
(42) Aubouy, M.; Guiselin, O.; Raphael, E. *Macromolecules* **1996**, 29, 7261−7268.
(43) Aubouy, M.; Dimeglio, J. M.; Raphael, E. *Europhys. Lett.* **1993**, *24*, 87−92.
(44) Hariharan, R.; Russell, W. B. *Langmuir* **1998**, *14*, 7104−7111.
(45) Ciprari, D.; Jacob, K.; Tannenbaum, R. *Macromolecules* **2006**, *39*, 6565−6573.